BIOCHEMISTRY
including biophysical chemistry & molecular biology

ARTICLE

pubs.acs.org/biochemistry

The Stability of Myocilin Olfactomedin Domain Variants Provides New Insight into Glaucoma as a Protein Misfolding Disorder

J. Nicole Burns, Katherine C. Turnage, Chandler A. Walker, and Raquel L. Lieberman*

School of Chemistry and Biochemistry, Georgia Institute of Technology, 901 Atlantic Drive Northwest, Atlanta, Georgia 30332-0400, United States

Supporting Information

ABSTRACT: Myocilin variants, localized to the olfactomedin (OLF) domain, are linked to early-onset, inherited forms of open-angle glaucoma. Disease-causing myocilin variants accumulate within trabecular meshwork cells instead of being secreted to the trabecular extracellular matrix of the eye. We hypothesize that, like in other diseases of protein misfolding, aggregation and downstream pathogenesis originate from the compromised thermal stability of mutant myocilins. In an expansion of our pilot study of four mutants, we compare 21 additional purified OLF variants by using a fluorescence stability assay and investigate the secondary structure of the most stable variants by circular dichroism. Variants with lower melting temperatures are correlated with earlier glaucoma diagnoses. The chemical chaperone trimethylamine *N*-oxide is capable of restoring the stability of most, but not all, variants to wild-type (WT) levels. Interestingly, three reported OLF disease variants, A427T, G246R, and A445V, exhibited properties indistinguishable from those of WT OLF, but an increased apparent aggregation propensity in vitro relative to that of WT OLF suggests that biophysical factors other than thermal stability, such as kinetics and unfolding pathways, may also be involved in myocilin glaucoma pathogenesis. Similarly, no changes from WT OLF stability and secondary structure were detected for three annotated single-nucleotide polymorphism variants. Our work provides the first quantitative demonstration of compromised stability among many identified OLF variants and places myocilin glaucoma in the context of other diseases of protein misfolding.

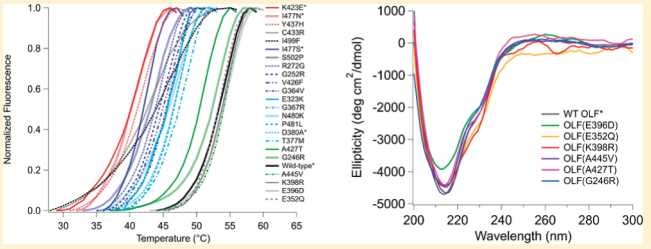

Glaucoma, a leading cause of blindness from retinal degeneration, is a heterogeneous disorder with complex traits, including an early-onset, inherited form closely linked to mutations in the gene encoding myocilin.[1] More than 70 glaucoma-causing mutations have been documented within the myocilin gene, predominantly within its olfactomedin (OLF) domain, from unrelated families of different racial and ethnic backgrounds.[2] Among several of its known intra- and extracellular locations in the eye and throughout the human body,[3,4] myocilin is found in high levels in the trabecular extracellular matrix (TEM), the region of the eye believed to regulate intraocular pressure.[5] Missense mutations leading to altered amino acid sequences result in its nonsecretion from[6] and intracellular sequestration within[7,8] trabecular meshwork cells. The molecular mechanism(s) by which a mutant myocilin leads to altered fluid flow[9] and increased intraocular pressure, a common risk factor for glaucoma,[10] is an active area of investigation.[4]

Clues about the molecular pathogenesis of myocilin glaucoma come from the cellular studies of mutant myocilins. Overexpressed myocilins have been shown to form toxic aggregates that induce an ER stress response[11,12] and, eventually, result in cell death.[12,13] In vitro, aggregates of mutant myocilin are not soluble in Triton X-100 (TX100),[14] and in several model cell systems, some secretion can be rescued when cells are cultured at 30 °C,[15−17] an experimental condition known to reduce the rates of cellular protein folding and accumulation of potentially toxic protein. For select mutants tested, the addition of nonspecific chemical chaperones such as glycerol, phenyl butyrate,[18] and trimethylamine *N*-oxide (TMAO)[19] also improves secretion. Finally, when cotransfected with wild-type (WT) myocilin, aggregates of hetero-oligomers are observed intracellularly, consistent with the general autosomal-dominant inheritance pattern observed for myocilin glaucoma.[20]

On the basis of these data, an attractive model for the pathogenesis of myocilin glaucoma involves a toxic gain-of-function for mutant myocilin in trabecular meshwork cells. In the ER, the proteostasis network assists in nascent polypeptide folding and carefully monitors the folded protein to ensure that only correctly folded proteins continue on the path to maturation and cellular trafficking; otherwise, the degradation process is initiated.[21] In the case of mutant myocilin, it may be the case that degradation pathways cannot keep up with the accumulation of newly synthesized mutant myocilins that are largely incompetent for secretion to the TEM, which leads to aggregation and ER stress that cannot be alleviated. Additional support for this pathogenesis proposal comes from the findings that glaucoma does not develop in myocilin knockout mice[22] or in individuals with premature stop codons that prevent translation of myocilin entirely.[23] Nevertheless, it is noted that the toxic gain-of-function hypothesis for

Received: February 14, 2011
Revised: May 24, 2011
Published: May 25, 2011

```
gi_3065674     228 -LKESPSGYLRSGEGDTGCGELVWVGEPLTLRTAETITGKYGVWMRDPKPTYPYTQETTWRIDT-VGTDVRQVFEYDLIS 305
gi_62632725    205 ---------QDGPADISGCGDLVWVENPEVHRKADSIAGKYGVWMQDPEAKEPYGPDMVWRIDS-VGSEVRQLFGYENMD 274
gi_74356501    214 -LKESPSGHPRNEEGGTGCGELVWVGEPITLRTAETITGKYGVWMRDPQATFPYTGETTWRIDT-VGTDIRQVFEYDHIR 291
gi_47522798    213 -LKESVSGHSGSEEGGSGCGELVWVGEPVTLRTAETITGKYGVWMRDPKATYPYTQETTWRIDT-VGTDIRQVFEYDRIS 290
gi_15077142    214 -LKENPSGRPRSKEGDKGCGALVWVGEPVTLRTAETIAGKYGVWMRDPKPTHPYTQESTWRIDT-VGTEIRQVFEYSQIS 291
gi_3845607     227 --LKNQSGHPRSKEGDKGCGVLMWVGEPVTLRTAETITGKYGVWMRDPKPTHPYTQETTWRIDT-VGTGIRQVFEYSQIS 303
gi_28453877    209 TEDESLFQPWSDFPSQDSCRDIIHVSEPFTVRGVG---NKIGAWFRDPLQDYI----KVYYAPFHNPRLTYQVDRFAHVA 281
Mutation                           *     *                 *           *

gi_3065674     306 QFMQGYPS---KVHILPRPLESTGAVVYSGSLYFQGAESRTVIRYELNTETVKAEKEIPGAGYHGQFPYSWGGYTDIDLA 382
gi_62632725    275 QLTRGFPT---KVLLLPESVESTGATMYKGSLYYQRRLSRTLIRYDLHAESIAARRDLPHAGFHGQFPYSWGGYTDIDLA 351
gi_74356501    292 QFTQGYPS---KVHVLPRPLESTGAVVYRGSLYFQAAESRTVLRYDLRTETLKAEKEIPGAGYHGQFPYSWGGYTDIDLA 368
gi_47522798    291 QFAQGYPS---KVHVLPRRLESTGAVVYQGSLYFQGASSRTVIRYELSTETLKAEKEIPGAGYHGQFPYSWGGYTDIDLA 367
gi_15077142    292 QFEQGYPS---KVHVLPRALESTGAVVYAGSLYFQGAESRTVVRYELDTETVKAEKEIPGAGYHGHFPYAWGGYTDIDLA 368
gi_3845607     304 QFEQGYPS---KVHVLPQALESTGAVVYAGSLYFQGAESRTVLRYELNTETVKAEKEIPGAGYHGQFPYAWGGYTDIDLA 380
gi_28453877    282 DFRGGTEYEHRYMLPTNLPAQGPGMVAYNGSLYYHAFQSRQIVRYDLENHTVVTTGEISDADI-----NIRGSPSAIDLA 356
Mutation                           *                             *           *  *  *      *  *

gi_3065674     383 VDEAGLWVIYSTDEAKGAIVLSKLNPENLELEQTWETNIRKQSVANAFIICGTLYTVSSYTSADATVNFAYDTGTGISKT 462
gi_62632725    352 IDENGLWAIYSTNKAKGAIVISQLDPHNLEVKGTWETKIRKTSVANAFMICGKLYTVASYTSPNTTVNYMFDTATSQGKA 431
gi_74356501    369 VDEIGLWVIYSTEAAKGAIVLSKLNPETLELEQTWETNIRKQSVANAFIICGTLYTVSSYSSPDATVNFAYDTGTGSSKA 448
gi_47522798    368 VDETGLWVIYSTEAAKGAIVLSKLNPENLELERTWETNIRKQSVANAFIICGTLYTVSSYSSPEATINFAYDTSTGSSKA 447
gi_15077142    369 VDESGLWVIYSTEEAKGAIVLSKLNPANLELERTWETNIRKQSVANAFVLCGILYTVSSYSSAHATVNFAYDTKTGTSKT 448
gi_3845607     381 VDESGLWVIYSTEETRGAIVLSKLNPENLELESTWETNIRKQSVANAFVICGILYTVSSYSSVHATINFAYDTNTGISKT 460
gi_28453877    357 VDELGLWAIYASVSDQTNTMISRLDPETLDVIETWVAPFPKYQAGSCFMVCGRLYCLSSFFSTDSTVELVYETSSNVFRV 436
Mutation                      * *                       *  **     *   *       *

gi_3065674     463 LTIPFKNRYKYSSMIDYNPLEKKLFAWDNLNMVTYDIKLSKM----------------- 504
gi_62632725    432 ISVPFKNRYRYNSMVDYNSAKRKLYAWDNYYMVSYSVRLGKQE---------------- 474
gi_74356501    449 LTVPFKNRYKYSSMIDYNPLERKLFAWDNFNMVSYDIKLSRL----------------- 490
gi_47522798    448 LTIPFKNRYEYSSMIDYNPLEKKLFAWDNFNMVTYDIRLSRM----------------- 489
gi_15077142    449 LTIPFTNRYKYSSMIDYNPLERKLFAWDNFNMVTYDIKLLEM----------------- 490
gi_3845607     461 LTIPFKNRYKYSSMVDYNPLERKLFAWDNFNMVTYDIKLSEM----------------- 502
gi_28453877    437 IDVLFDIRFGEMMSLKYNPRDQKLYGWDNGHQVVYDLTFDPPARSQLLPTDTNIPLNLQ 495
Mutation                        *  **               *  *
```

Figure 1. Multiple-sequence alignment of the myocilin OLF domain and nonocular amassin OLF domain. The alignment includes myocilin OLF domains from *Homo sapiens* (gi accession number 3065674), *Danio rerio* (gi accession number 62632725), *Bos taurus* (gi accession number 74356501), *Sus scrofa* (gi accession number 47522798), *Mus musculus* (gi accession number 15077142), and *Rattus norvegicus* (gi accession number 3845607) and the amassin OLF domain from *Strongylocentrotus purpuratus* (gi accession number 28453877). Blue represents similar residues, red represents identical residues, and asterisks represent the site of mutation in this study. The alignment was generated using PROMALS3D.[70]

myocilin glaucoma, particularly ER sequestration and stress followed by apoptosis, does not converge with all of the available data for WT behavior in cells[24−27] or observations of mutant myocilin effects in transgenic mice;[7,8] thus, additional work in the area is needed.

The purpose of this study is to compare the thermal stabilities of numerous OLF missense mutants with WT OLF to lend further credibility for the categorization of myocilin glaucoma as a protein misfolding disorder. This large disease superfamily includes p53-related cancers,[28] SOD1-related amyotrophic lateral sclerosis (ALS),[29] certain subtypes of diabetes,[30] lysosomal storage disorders such as Gaucher disease,[31−33] among others. A feature common to these disorders is a missense mutation(s) in a gene that leads to altered protein behavior, aberrant cellular or extracellular activity, and detrimental downstream effects that ultimately manifest in disease. Complementary to cellular studies, animal model studies, genetic analysis, and clinical diagnosis, biophysical analysis of the behavior of purified mutant proteins in vitro is an integral part of comprehending the underlying genotype−phenotype relationships that contribute to pathogenesis.

The disease-causing mutants selected for this stability study (see Figure 1), which together comprise ∼40% of all reported glaucoma-causing myocilin mutations,[2] have been evaluated previously for aggregate solubility in TX100[14,34] and/or temperature-sensitive secretion.[16,17] We also studied three amino acid-altering single-nucleotide polymorphism (SNP) variants, which appear in at least 1% of the population.[35] These OLF variants are presumed to be benign, and one had been investigated in the solubility assay. Two major disadvantages of the study of OLF, especially compared to p53 or SOD1, are the inability to postulate a correlation between mutation and function and to categorize mutations by mapping their location on the three-dimensional structure of the protein. Unfortunately, homology modeling with distantly related structural models covers only half of the available OLF sequence, and in these models, the cysteine residues known to form a disulfide bond[36,37] are not proximal to each other (not shown). Nevertheless, the new stability data set presented here provides the first quantitative demonstration of compromised stability among most, but not all, reported OLF variants and, combined with results of previous assays and age of glaucoma diagnosis, expands the possible disease mechanisms for myocilin glaucoma in the context of a protein misfolding disorder.

EXPERIMENTAL PROCEDURES

Expression and Purification of the Maltose Binding Protein−OLF Fusion (MBP−OLF) and Corresponding Mutants. The plasmid for MBP−OLF was cloned as we described previously.[36] Mutant MBP−OLFs were generated by site-directed mutagenesis (QuikChange, Stratagene) using the primers listed in Table S1 of the Supporting Information. Mutated plasmids, verified by DNA sequencing (MWG Operon),

were transformed into Rosetta-Gami 2(DE3)pLysS cells (Novagen), cultured, induced, and harvested, as described previously.[36] Procedures for isolation and purification also followed closely procedures described in ref 36. Briefly, after lysis with a French press and ultracentrifugation to remove all cell debris and insoluble materials, MBP−OLFs were purified using an amylose affinity column and further fractionated into two major species by size exclusion chromatography (SEC), namely, cytosolic aggregates that elute in the void volume and a monomeric species that elutes at the expected retention volume for the fusion protein, ~72 kDa (Figure S1 of the Supporting Information). The intensity of the monomer peak was highly variable among the mutants described in this study (Figure S1 of the Supporting Information) but consistent within preparations of each mutant, as noted previously.[36] Two variants, P370L and W286R, could be isolated only as aggregates; an insufficient quantity of monomer could be isolated for further study. SEC results were normalized by first subtracting the baseline absorbance and then dividing by the highest absorbance value observed in the chromatograph. Purified MBP−OLFs used in experiments were stored continuously at 4 °C and used within 3 days.

Cleavage of MBP−OLF to isolate OLF proteins for circular dichroism (CD) experiments (below) was accomplished by overnight (~16 h) incubation at 37 °C (WT MBP−OLF and mutants G246R, E352Q, E396D, K398R, A427T, and A445V) or room temperature (mutants V426F, Y437H, and I499F) with Factor Xa (New England Biolabs or Roche) in 50 mM Tris (pH 8) or 50 mM Hepes (pH 7.5), 100 mM NaCl, and 5 mM $CaCl_2$. Cleaved OLF variants were fractionated from uncleaved material and MBP by amylose affinity purification followed by fractionation of the unbound material by using a Superdex 75 GL column (GE Healthcare) at 4 °C, to remove all traces of Factor Xa. Cleaved OLFs were subjected to CD analysis immediately after purification.

Differential Scanning Fluorimetry (DSF). The stability of OLF variants in the context of MBP−OLF was assessed using a sensitive, quantitative, and relatively high-throughput SYPRO Orange (Invitrogen) fluorescence melt assay that follows the increase in accessible hydrophobic regions as a protein is unfolded.[36] The addition of 50 mM maltose, which binds to and stabilizes MBP only, serves to shift the melting temperature (T_m) of MBP completely out of the range for OLF (67 °C) and conveniently allows an independent, and simultaneous, measurement of the T_m for MBP and OLF.[36] MBP−OLF variants were subjected to this assay in at least triplicate using a Step One Plus (Applied Biosciences) real time (RT) polymerase chain reaction (RT-PCR) instrument, as described previously.[36] Data were analyzed using Graphpad Prism as detailed in ref 38 to identify the midpoint of the transition, the definition of T_m.

The DSF assay was also used to monitor the responses of OLF variants to 3 M TMAO (Figure S2 of the Supporting Information), an osmolyte found previously to be stabilizing for both the WT and select mutants.[36] TMAO is a small molecule thought to exert its stabilizing influence mainly on the peptide backbone rather than the side chain[39] and thus would be expected to stabilize all variants to the same extent. The inability of 3 M TMAO to rescue proteins to WT levels (without TMAO) was used as a guideline to cluster the least stable OLF variants (see below).

Circular Dichroism (CD). To compare the secondary structure of selected cleaved OLF variants (5−10 μM) with that of WT OLF, CD spectra were recorded at room temperature on a Jasco J-810 CD spectropolarimeter. Samples were prepared in 10 mM Na/K phosphate and 0.2 M NaCl (pH 7.2) and placed in a 0.1 cm cell for data collection. Thirty to forty consecutive scans ranging from 200 to 300 nm, using a bandwidth of 1 nm at a continuous scanning rate of 500 nm/min, were averaged for each sample. Each spectrum was background-subtracted and converted to mean residue ellipticity: $[\theta] = (M_{res}\theta_{obs})/(10dc)$, in which M_{res} equals 112.9 and is the mean residue ellipticity (based on protein sequence), θ_{obs} is the observed ellipticity in degrees at a specific wavelength, d is the path length in centimeters, and c is the protein concentration in grams per milliliter. Melts for V426F, Y437H, and I499F variants were conducted in duplicate and were analyzed using Boltzmann sigmoid analysis as described previously.[40]

Statistical Analysis. Statistical analyses were performed using Graphpad Prism. Where appropriate, Pearson's correlation is reported and considered significant at a level greater than $\alpha = 0.05$. Unpaired and one-sample t tests were also conducted, and two-tailed p values of <0.05 were considered significant. For the correlation of age of diagnosis with T_m, the average T_m values for explicitly reported diagnosis ages were included for analysis. Otherwise, no reported data were excluded from Table 1 prior to analysis.

RESULTS

All of the monomeric OLF mutants tested in this study unfold in the T_m range of 40−55 °C (Table 1 and Figure 2) with a precision of ~1 °C. We estimate the accuracy of the DSC T_m measurement to within 2 °C. This evaluation is based on previous work comparing T_m results for WT OLF obtained by DSF with T_m values obtained by traditional biophysical techniques such as CD and tryptophan fluorescence melts[40] as well as in this work, in which the unfolding of three OLF disease-causing variants [V426F, Y437H, and I499F (Figure S3 and Table S2 of the Supporting Information)] was examined by CD. Spectra of V426F, Y437H, and I499F are similar to that of WT OLF (Figure S3a of the Supporting Information), namely, the β-sheet signature at ~214 nm and the β-turn shoulder at ~230 nm,[40] and for melts, minor deviations were observed in T_m of the main 214 nm feature compared to DSF values (Table S2 of the Supporting Information). A limitation of the accuracy of T_m values obtained for aggregation-prone OLF by any method is that conditions for reversibility of the transition have not yet been identified. However, in addition to using different methods to measure the T_m, the scan rate dependence for several techniques has been examined,[40] and experiments described here were conducted at the same slow rate consistent with unfolding under microscopic equilibrium conditions.

Least Stable Variants (group A). The least stable OLF variants include K423E, I477N, and Y437H, with T_m values of ~40 °C by DSF (ref 36, Table 1, and Figure 2, group A). Included in group A are also the two variants for which no monomeric protein could be isolated. The stability of the three isolated variants could not be rescued to WT levels by TMAO (Table 1 and Figure S2 of the Supporting Information), but the three variants are folded proteins with minimal perturbation in secondary structure observed by CD (see ref 36 and Figure S3 of the Supporting Information). In relation to previous results using TX100 solubility to characterize myocilin aggregates (Table 1), these OLF mutants were found to generate insoluble aggregates.

Table 1. Compilation of Data for Myocilin Variants from This Study and Previous Studies[a]

Group	Mutation			T_m			Solubility Assay[b]	Secretion Assay[c]		Age(s) of Diagnosis[d]	References[d]
				Protein only	+3M TMAO	ΔT_m		37 °C	30 °C		
A	P	370	L	NA	NA	NA	I	N	+/-	12, 12, 10.5	(*34*), (*56*), (*42*)
	W	286	R	NA	NA	NA	NA	N	N	NA (pop.)	(*57*)
	I	477	N	40.1±0.8	50.1±0.8	9.9	I	N	+/-	26, 18, 18, Pop.	(*34*), (*56*), (*58*), (*57*)
	K	423	E	40.5±0.1	48.8±0.7	8.3	I	N	N	19, 33, 30	(*59*), (*60*), (*43*)
	Y	437	H	41.4±0.1	50.4±1.1	9.0	I	N	+/-	NA (pop.), NA (pop.), 8-41	(*57*), (*61*), (*41*)
B	I	477	S	41.9±0.5	52.7±0.8	10.7	I	N	+++	33	(*42*)
	C	433	R	42.6±0.4	52.2±0.6	9.6	I	N	N	15, 38	(*62*)
	S	502	P	43.0±0.1	52.9±0.2	9.9	I	N	N	19	(*63*)
	I	499	F	44.4±0.3	56.3±0.3	11.9	PI	+/-	+++	28, 29, 31	(*34*), (*64*), (*42*)
	R	272	G	44.7±0.2	51.7±0.6	7.0	NA	N	++	33	(*34*)
	G	252	R	44.8±0.7	55.6±0.8	10.8	I	N	+++	26, 26	(*34*), (*56*)
	V	426	F	45.1±0.4	56.1±0.8	11.0	I	+/-	+++	21, 26	(*34*), (*56*)
	G	364	V	45.5±0.2	56.7±0.2	11.2	PI	+	+++	NA (pop., fam.)	(*57*), (*61*)
	E	323	K	45.6±0.4	57.5±0.5	11.9	I	+/-	+++	19, 19	(*34*), (*56*)
	G	367	R	45.7±0.1	56.3±0.3	10.6	I	N	+++	32, 34	(*65*), (*43*)
	N	480	K	46.1±0.3	52.2±0.8	6.1	I	+/-	++	30/35/32, 30/34/40	(*42*), (*66*)
	P	481	L	46.6±0.1	53.0±0.8	6.4	I	N	++	33, NA (pop.)	(*43*), (*57*)
	D	380	A	46.7±0.5	55.6±0.9	8.9	PI	+/-	+++	21	(*63*)
	T	377	M	47.7±0.2	60.6±0.7	12.9	PI	+	+++	38, 52, 40, NA (pop.)	(*34*), (*65*), (*67*), (*57*)
C	A	427	T	50.5±0.2	61.1±0.4	10.6	S	+++	NA	73	(*43*)
	G	246	R	52.7±0.5	60.8±0.7	8.1	I	N	++	20	(*42*)
	Wild-type			52.7±0.8	64.1±0.7	11.4	S	+++	NA	--	--
	K	398	R	53.8±0.2	62.2±0.2	11.9	S	NA	NA	rs56314834[e]	(*57*), (*68*), (*34*), (*43*), (*69*), (*66*)
	E	396	D	53.1±0.1	61.9±0.1	12.3	NA	NA	NA	rs61730975[e]	NA
	A	445	V	54.2±0.2	63.2±0.6	9.0	S	+++	NA	63, NA (pop.)	(*43*), (*57*)
	E	352	Q	54.9±0.5	63.1±0.4	9.0	NA	NA	NA	rs61745146[e]	NA

[a] Variants are listed in order of melting temperature (T_m). Abbreviations: NA, not available; −, not applicable; I, insoluble; PI, partially insoluble; S, soluble; N, no secretion; +/−, little secretion; +, ++, and +++, increasing amounts of secretion as defined in ref 17. [b] Data from ref 14 and/or ref 34. [c] Data from ref 16 and/or ref 17. [d] Commas separate ages reported in order of references, with a slash indicating multiple ages reported, pop. indicating the population study with no age of diagnosis provided, and fam. indicating a familial study with no age of diagnosis provided. [e] Accession numbers for Database of Single Nucleotide polymorphisms (dbSNP, Build ID 131), available from: http://www.ncbi.nlm.nih.gov/SNP.

Likewise, the variants in group A showed no secretion from cells at 37 °C and little, if any, secretion at 30 °C. Finally, these variants are associated with the overall earliest ages of glaucoma diagnosis. The mutation associated with the earliest age of diagnosis, 10 years, is P370L. The I477N and K423E mutants have been diagnosed as early as ages 18 and 19, respectively. For Y437H, the range of diagnosis is 8−41 years.[41]

Notably, K423 and Y437 are strictly conserved among myocilins from related mammals such as mice, rats, fish, and cows (Figure 1). Given the fact that the mutation results in an amino acid similar in size to the WT amino acid, side chain interactions and properties are likely important at these sites. For example, as indicated by the different melt profiles observed for 214 and 229 nm (Figure S3c of the Supporting Information, T_m values in Table S2), Y437H melts in a less cooperative manner than other variants (Figure S3b,d of the Supporting Information) and WT OLF,[40] suggestive of non-native interactions. Likewise, K423 may be located within the interior of the protein, where positive charge would be stabilized by a neighboring anionic charge. By contrast, I477 is not conserved (Figure 1). Val and Leu are found in this position in *D. rerio* and the nonocular OLF domain of *S. purpuratus* amassin, respectively, suggesting I477 is located in a hydrophobic pocket that cannot accommodate a polar residue such as Asn.

Moderately Stable Variants (group B). The majority of OLF variants lie in the midrange of stability, more stable than the most severe mutants and statistically less stable than WT, at T_m values between 42 and 48 °C (Table 1, Figure 2, group B, $p < 0.0001$). Variants in this group include changes in size, polarity, and charge, and overall, in the absence of knowledge about how the mutations map on the three-dimensional structure of OLF, it is not straightforward to reconcile the effects of certain mutations on protein stability. For example, charge inversion in E323K appears to cause an only moderately destabilizing effect, but as noted above, the opposite charge inversion in K423E results in a severely compromised protein. Similarly, substitution of I477 with a Ser, a small polar residue, results in a low-stability protein, whereas a less detrimental effect is seen when the similarly small G367 is replaced with the large, positively charged, Arg.

All group B variants can be rescued to at least WT stability by the addition of 3 M TMAO (Table 1), and most OLF mutants in this range unfold with sharp transitions, suggestive of two-state transitions. Two exceptions are C433R and I499F, which exhibit shallower unfolding transitions, implicating possible intermediates in the unfolding pathway. In the case of the invariant cysteine at position 433 (Figure 1), the single disulfide bond[36,37] is disrupted and could result in a change in the unfolding pathway. We note, however, that the C433R variant is a well-behaved monomer in solution; no heterodimerization by oxidation of the lone cysteine 245 has been observed (not shown), suggesting that the WT OLF disulfide bond is not surface-accessible. By

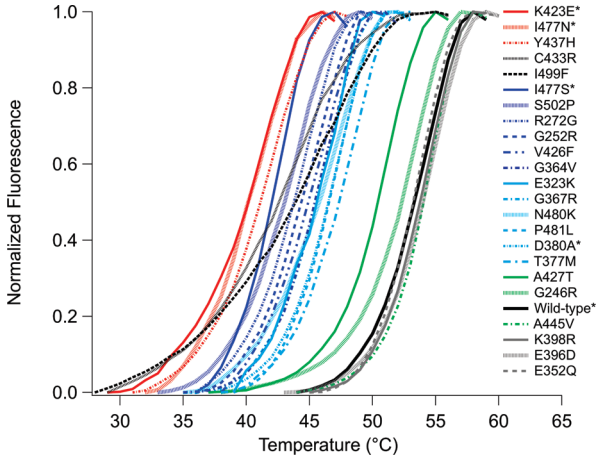

Figure 2. Melting thermograms for myocilin OLF variants: (solid black line) WT OLF, (red lines) group A, (blue and dashed black lines) group B, and (green and gray lines) group C. Note two dashed black curves corresponding to C433R and I499F deviate from the apparent two-state transition. Asterisks denote curves published in ref 36. No thermograms were obtained for W286R or P370L.

contrast, the observed result for I499F may be an artifact of interactions with the Sypro Orange dye. Although the T_m values measured by DSF and CD (Table S2 of the Supporting Information) are similar to one another, a more cooperative transition is observed by CD, with no obvious difference in T_m measured at either of the two spectral features (Figure S3d of the Supporting Information). In addition, this region of OLF is not part of the identified core structural domain.[40]

Finally, in terms of the solubility of aggregates, most myocilin variants in this group were previously found to produce insoluble aggregates according to the TX100 assay (see Table 1), with the exception of four variants that partitioned into both the soluble and insoluble fractions: I499F and G364V as well as D380A and T377M. The latter two variants are the most stable of group B; their behavior is consistent with a general trend of increasing TX100 solubility with T_m (see Discussion). Group B variants also exhibit little or no secretion at 37 °C but, with the exception of C433R and S502P, are secreted to some degree at 30 °C (see Table 1). In terms of age of diagnosis, there is a wide variation between 15 and 52 years, with an average of 29 years.

Most Stable Variants (group C). Of the annotated disease-causing mutants we studied, three (A427T, G246R, and A445V) unfold within 2 °C of WT OLF (T_m = 52.7 ± 0.8 °C[36]) in the absence of TMAO, indicating they have WT-like stability ($p > 0.8$). These variants were further probed for structural changes by CD and found to be comparable to WT OLF (Figure 3a). The ratio of aggregate to monomer isolated as part of the purification procedure is higher for these three mutants than for WT, however (Figure 3b, Figure S1 of the Supporting Information, and Discussion). The three SNP variants (K398R, E396D, and E352Q) that were identified through genome-wide sequencing efforts and are not associated with glaucoma exhibit stability that is similar to or exceeds that of WT OLF. Comparison of the CD spectra of cleaved OLF SNP variants reveals no significant differences in structure (Figure 3a). In contrast to the other WT-like disease-causing mutants, the ratio of aggregate to monomer for SNPs is at least as favorable as that of WT OLF (Figure 3c). Finally, group C OLF variants exhibit WT OLF behavior in the aggregate solubility and cell secretion assays,

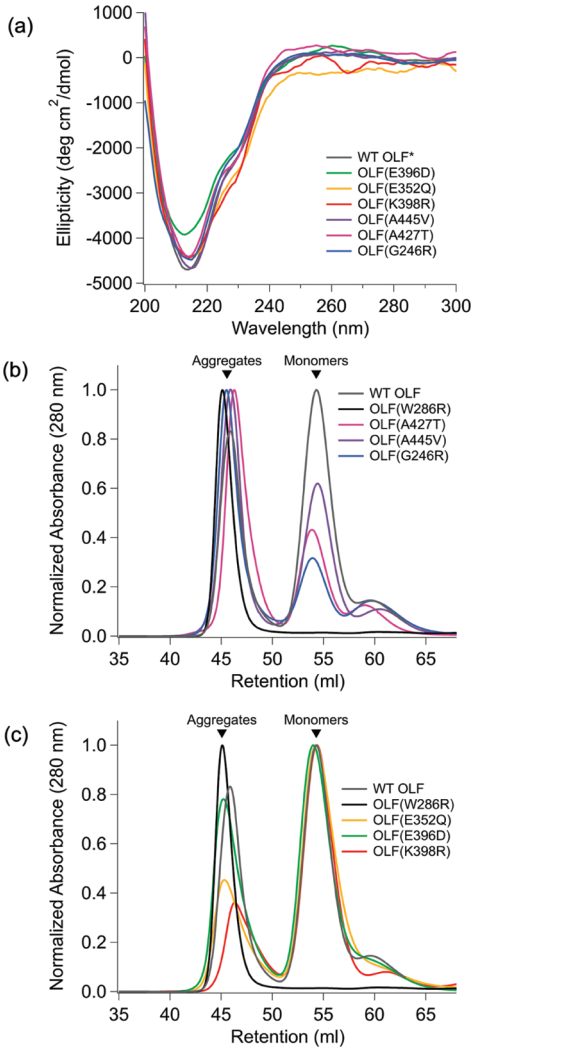

Figure 3. Features of most stable OLF variants. (a) Circular dichroism spectra for group C variants. The asterisk denotes the spectrum for WT OLF reported in ref 40. (b) Comparison of relative aggregate and monomer isolated for disease-causing variants in group C with W286R and WT OLF by size exclusion chromatography. (c) Comparison of relative aggregate and monomer isolated for SNP variants with WT OLF by size exclusion chromatography. Each trace has been normalized.

namely, high solubility in TX100 and ample secretion at 37 °C (Table 1). The main outlier in this group is G246R (see below). This group of variants also exhibits a broad range of age of diagnosis with an average of 52 years with a span from 20 to 73 years.

DISCUSSION

Trends. Taken together (Table 2), group A comprises the least stable OLF variants that form largely insoluble aggregates, cause the most severe cellular effects, and, overall, have the earliest diagnosis of glaucoma. Those variants in group B are in the intermediate range of glaucoma cases in terms of stability, age of diagnosis, and cellular defects. Mutant proteins in this group correspond to myocilin aggregates that are soluble or partially soluble in the TX100 assay and mutant myocilin that can be secreted to some extent from cells cultured at 30 °C. For group C, variants exhibit WT levels of stability and cellular secretion, are soluble in TX100,

Table 2. Overall Trends of OLF Variant Stability

	T_m	solubility of aggregates in TX100	cell secretion	average age of diagnosis
group A	lowest	insoluble	limited at 30 °C	19
group B	moderate	insoluble or partially insoluble	some at 30 °C	29, highly variable
group C	wild-type	largely soluble	secretion at both 37 and 30 °C	52

and receive the latest diagnosis of glaucoma. All OLF variants we have examined to date by CD retain a secondary structure similar to that of WT OLF.

With a substantial protein stability data set now in hand, the statistical significance of specific trends can be evaluated. First, given the caveat that "age of diagnosis" is the best available proxy for ill-defined parameters such as "age of onset" and "disease severity" for glaucoma patients, the parameter is positively correlated with T_m [correlation coefficient of 0.54, statistically non-zero slope of 0.154, $p < 0.0005$ (Figure 4a)]. The age of diagnosis is expected to vary among patients because (a) glaucoma is painless and can go unnoticed until loss of visual field occurs (asymptomatic patients under 40 years of age are rarely examined by ophthalmologists[10]) and (b) age data are only available for a subset of recorded variants. In addition, the age of diagnosis for a patient harboring WT OLF is not defined, but the trend is supported if WT OLF (52.7 °C) is included for an age of 40 years, the threshold for adult-onset open-angle glaucoma.[1] Second, in terms of aggregates categorized by the TX100 assay, there is a difference between the T_m of variants with insoluble or partially insoluble aggregates and the T_m of variants with soluble aggregates [$p = 0.0002$ and 0.0009, respectively (Figure 4b)]. Similarly, poorly secreted myocilins at 37 or 30 °C exhibit lower OLF T_m values than their well-secreted counterparts [for non-secretion vs secreted at 37 °C, $p = 0.0022$, and for 30 °C, $p = 0.01$ (Figure 4c,d)]. Overall, correlations between T_m and aggregation or nonsecretion are consistent with the definition of T_m, which relates to the relative balance of unfolded protein compared to folded at a given temperature; the higher the proportion of unfolded protein, the greater the exposure of interior hydrophobic and aggregation-prone residues.

Outliers. In spite of trends for most myocilin variants, the presence of several categories of outliers illustrates the nuanced effects of mutations on the biophysical properties of OLF that may contribute to myocilin glaucoma pathogenesis. First, three amino acid substitutions observed in the moderately stable group, R272G, N480K, and P481L, result in a poor response to stabilization by TMAO. On average, 3 M TMAO exerts an impressive and consistent 10 °C improvement in stability versus WT and nearly all mutant OLFs, but these outliers lie well outside the lower boundary for the 95% confidence interval and one standard deviation below the mean (Figure 4e). Sequence alignment with myocilin from other organisms (Figure 1) reveals that these three positions are highly conserved, suggesting they are key to the structural integrity of OLF. Among the six species aligned, R272 is substituted only once, in *D. rerio* (Gln), and the other two residues are invariant. It is possible that an interaction utilizing the side chain of Arg or Asn contributes significantly to overall stability, and effects of TMAO on the polypeptide main chain cannot compensate for the loss of either of these interactions. In addition, conformationally restrictive Pro residues are typically found in specialized roles in the polypeptide backbone that cannot be filled by a Leu substitution.

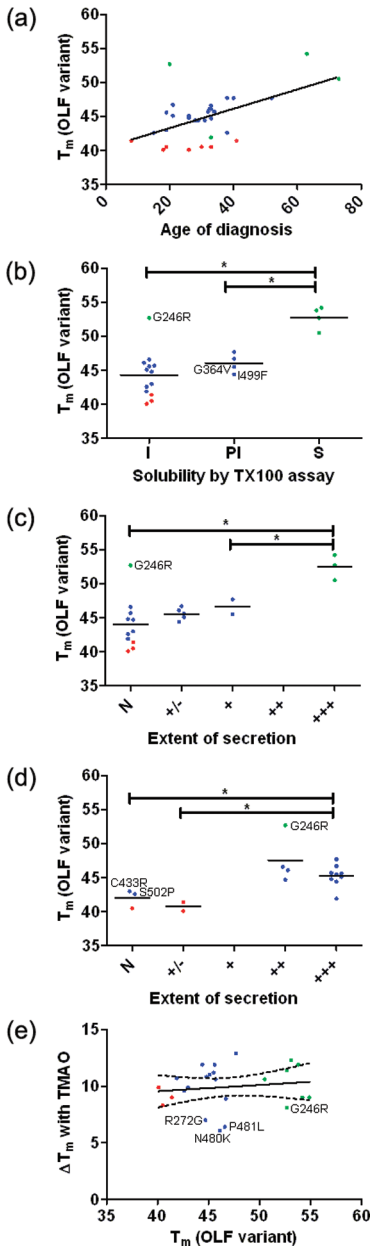

Figure 4. Statistical analyses conducted in this study. (a) Correlation between T_m of an OLF variant and the age of glaucoma diagnosis. (b) Significance of T_m differences and aggregate solubility using the TX100 assay. (c and d) Significance of T_m differences and extent of secretion from cells cultured at 37 and 30 °C, respectively. For panels b−d, see the symbol definitions in Table 1. (e) ΔT_m for each OLF variant with the addition of 3 M TMAO plotted as a function of T_m without TMAO. Dashed lines indicate 95% confidence intervals, and the slope does not statistically deviate from zero ($p > 0.5$). Red, green, and blue colors indicate variants found in groups as defined in Table 1; outliers discussed in the text are labeled. Asterisks denote a statistical difference with p of <0.05 as described in text.

dx.doi.org/10.1021/bi200231x |*Biochemistry* 2011, 50, 5824–5833

Second, aggregates of the moderately stable variants G364V and I499F are partially soluble in the TX100 assay, whereas all but the most stable variants in this group are insoluble in the assay. Another common factor between these two variants is their low, but detectable, secretion from cells at 37 °C. In the well-studied nonocular myocilin homologue, *S. purpuratus* amassin, G364 is replaced with Asp, suggesting that in principle, a smaller side chain, such as Val, may be accommodated. In the case of the I499F variant, other hydrophobic residues such as Val (*D. rerio*) and Leu (*S. purpuratus*) are tolerated in this position, suggesting Phe should be tolerated as well. Genetic evidence consistent with the finding of favorable solubility and secretion behavior for I499F is incomplete penetrance; within a single family, only seven of nine individuals harboring this mutation were diagnosed with glaucoma.[42] However, a molecular rationale for favorable solubilization and secretion behavior of these two moderately stable OLF variants is not apparent and remains an open area for further investigation.

Third, unlike all other moderately stable variants that exhibit some secretion from cells cultured at 30 °C, inexplicably, C433R and S502P do not. One possibility for this phenotype is that the resulting aggregates are particularly harmful. Any unfolding intermediates (see Results and Figure 2) in C433R may stably expose part of its hydrophobic core that could inadvertently recruit other nascent polypeptides prior to aggressively forming inclusions, for example. For S502P, alteration to the inflexible Pro residue may compromise the structural integrity of this C-terminal region,[40] although smaller and larger amino acids, charged and hydrophobic, appear to be tolerated in this position (see Figure 1).

Lastly, it is curious that certain mutants exhibit WT OLF stability, CD spectral features, aggregate solubility, and cell secretion profile. At first glance, it might be tempting to dismiss disease-causing group C variants as mislabeled. To the best of our knowledge and unlike the SNP variants, A427T and G246R have been reported just once, A445V has been reported twice (Table 1), and individuals reported to harbor the A427T or A445V substitution were diagnosed at 63 or 73 years of age, respectively,[43] outside the threshold for early-onset glaucoma[1] (Table 1). However, upon closer inspection, there are differences between WT OLF and G246R, A427T, and A445V that suggest they may be pathogenic. First, G246R is an outlier in stabilization enhancement by TMAO (Figure 4e); other variants with Gly to Arg mutations (G252R and G367R) are less stable but do not share this feature. G246R is also an outlier in terms of the TX100 (Figure 4b) and cell secretion assays (Figure 4c,d). In addition, although the phenomenon is not understood, all OLF variants expressed and purified to date in *E. coli* exhibit a characteristic, noninterconverting, and reproducible ratio of void volume-to-monomer peak ratio (see ref 36 and Figure S1 of the Supporting Information), with a higher relative yield of monomer for nonpathogenic compared to disease-causing variants. The SEC profiles for G246R, A427T, and A445V follow the less favorable ratio similar to disease-causing variants, and not that of the SNPs (Figure 3b,c). In summary, these variants harbor defects that are apparent by SEC but not protein stability measurements, the details of which will need to be investigated further.

Comparison to Other Protein Conformational Disorders. The findings for OLF variants in this study fit well with observations in other diseases of protein misfolding in which pathogenic variants exhibit compromised thermal stability, as well as impaired biological function, changes in kinetics of folding, and/or changes in the folding pathway. For example, more than 150 temperature-sensitive, oncogenic p53 mutants have been identified.[44−46] However, some mutations localized to a loop in p53 weaken its DNA binding, an activity critical to its function as a transcription factor, without appreciably destabilizing the overall protein.[46] The specifics of the mutation in p53 correlate with breast cancer prognosis and response to treatment.[47] Similarly, numerous,[29] but not all, ALS-provoking SOD1 mutations alter protein stability.[48] One of the most prevalent SOD1 variants found in North America, A4V, is an example of a nondestabilized variant.[49] Mapped onto the SOD1 structure, pathogenic mutations in the main β-barrel typically lead to destabilized SOD1, whereas variants on the metal binding loop do not affect protein stability.[49] Notably, there is limited consensus about the mechanism by which a particular SOD1 mutant becomes aggregation-prone and pathogenic.[50] For example, changes in the net repulsive charge on SOD1 have been shown to trigger[51] or be protective of[50,52] pathogenic behavior. In addition, it is unclear whether aggregates are even the toxic species.[53] Finally, in neonatal onset diabetes mellitus, mutations that introduce an additional cysteine residue in proinsulin[30] lead to disulfide shuffling and kinetic trapping of misfolded intermediates,[54] yet non-cysteine missense mutations in proinsulin, located in a region not even present in mature, processed, insulin, can alter folding efficiency.[55]

In summary, this study of OLF variants reveals general relationships among protein stability, age of diagnosis, and protein behavior, and identifies notable outliers, including variants with traits indistinguishable from those of WT. These complexities are paralleled in other protein conformational disorders and should prompt further work to assess the contribution of biophysical properties other than protein stability, such as folding pathways or kinetics, in myocilin glaucoma. In the long term, complementary functional and structural studies will also be required to fully comprehend the effects of mutations on the OLF domain of myocilin, which together may ultimately allow therapeutic intervention.

■ ASSOCIATED CONTENT

Supporting Information. Figures S1−S3 and Tables S1 and S2. This material is available free of charge via the Internet at http://pubs.acs.org.

■ AUTHOR INFORMATION

Corresponding Author

*E-mail: raquel.lieberman@chemistry.gatech.edu. Phone: (404) 385-3663. Fax: (404) 894-2295.

Funding Sources

This work was supported by grants from the Glaucoma Research Foundation, the American Health Assistance Foundation, and the National Institutes of Health (R01EY021205); a Pew Scholar in the Biomedical Sciences award to R.L.L.; and a National Science Foundation Research Experiences of Undergraduates in Chemistry at Georgia Institute of Technology (0851780) award to C.A.W.

■ ACKNOWLEDGMENT

We gratefully acknowledge the Parker H. Petit Institute for Biosciences Core Facility for access to the RT-PCR instrument and to the Hud lab for use of their CD spectropolarimeter.

■ ABBREVIATIONS

ALS, amyotrophic lateral sclerosis; CD, circular dichroism; DSF, differential scanning fluorimetry; ER, endoplasmic reticulum; MBP, maltose binding protein; OLF, olfactomedin; SEC, size exclusion chromatography; SNP, single-nucleotide polymorphism; TEM, trabecular extracellular matrix; T_m, melting temperature; TMAO, trimethylamine *N*-oxide; TX100, Triton X-100.

■ REFERENCES

(1) Kwon, Y. H., Fingert, J. H., Kuehn, M. H., and Alward, W. L. (2009) Primary open-angle glaucoma. *N. Engl. J. Med. 360*, 1113–1124.

(2) Gong, G., Kosoko-Lasaki, O., Haynatzki, G. R., and Wilson, M. R. (2004) Genetic dissection of myocilin glaucoma. *Hum. Mol. Genet. 13*, R91–R102.

(3) Tamm, E. R. (2002) Myocilin and glaucoma: Facts and ideas. *Prog. Retinal Eye Res. 21*, 395–428.

(4) Resch, Z., and Fautsch, M. (2009) Glaucoma-associated myocilin: A better understanding but much more to learn. *Exp. Eye Res. 88*, 704–712.

(5) Tamm, E. R., Russell, P., Epstein, D. L., Johnson, D. H., and Piatigorsky, J. (1999) Modulation of myocilin/TIGR expression in human trabecular meshwork. *Invest. Ophthalmol. Visual Sci. 40*, 2577–2582.

(6) Jacobson, N., Andrews, M., Shepard, A. R., Nishimura, D., Searby, C., Fingert, J. H., Hageman, G., Mullins, R., Davidson, B. L., Kwon, Y. H., Alward, W. L., Stone, E. M., Clark, A. F., and Sheffield, V. C. (2001) Non-secretion of mutant proteins of the glaucoma gene myocilin in cultured trabecular meshwork cells and in aqueous humor. *Hum. Mol. Genet. 10*, 117–125.

(7) Senatorov, V., Malyukova, I., Fariss, R., Wawrousek, E. F., Swaminathan, S., Sharan, S. K., and Tomarev, S. (2006) Expression of mutated mouse myocilin induces open-angle glaucoma in transgenic mice. *J. Neurosci. 26*, 11903–11914.

(8) Zhou, Y., Grinchuk, O., and Tomarev, S. I. (2008) Transgenic mice expressing the Tyr437His mutant of human myocilin protein develop glaucoma. *Invest. Ophthalmol. Visual Sci. 49*, 1932–1939.

(9) Wilkinson, C. H., van der Straaten, D., Craig, J. E., Coote, M. A., McCartney, P. J., Stankovich, J., Stone, E. M., and Mackey, D. A. (2003) Tonography demonstrates reduced facility of outflow of aqueous humor in myocilin mutation carriers. *J. Glaucoma 12*, 237–242.

(10) Weinreb, R. N., and Khaw, P. T. (2004) Primary open-angle glaucoma. *Lancet 363*, 1711–1720.

(11) Wang, L., Zhuo, Y., Liu, B., Huang, S., Hou, F., and Ge, J. (2007) Pro370Leu mutant myocilin disturbs the endoplasm reticulum stress response and mitochondrial membrane potential in human trabecular meshwork cells. *Mol. Vision 13*, 618–625.

(12) Carbone, M. A., Ayroles, J. F., Yamamoto, A., Morozova, T. V., West, S. A., Magwire, M. M., Mackay, T. F. C., and Anholt, R. R. H. (2009) Overexpression of myocilin in the *Drosophila* eye activates the unfolded protein response: Implications for glaucoma. *PLoS One 4*, e4216.

(13) Yam, G. H.-F., Gaplovska-Kysela, K., Zuber, C., and Roth, J. (2007) Aggregated myocilin induces russell bodies and causes apoptosis: Implications for the pathogenesis of myocilin-caused primary open-angle glaucoma. *Am. J. Pathol. 170*, 100–109.

(14) Zhou, Z., and Vollrath, D. (1999) A cellular assay distinguishes normal and mutant TIGR/myocilin protein. *Hum. Mol. Genet. 8*, 2221–2228.

(15) Liu, Y., and Vollrath, D. (2004) Reversal of mutant myocilin non-secretion and cell killing: Implications for glaucoma. *Hum. Mol. Genet. 13*, 1193–1204.

(16) Vollrath, D., and Liu, Y. (2006) Temperature sensitive secretion of mutant myocilins. *Exp. Eye Res. 82*, 1030–1036.

(17) Gobeil, S., Letartre, L., and Raymond, V. (2006) Functional analysis of the glaucoma-causing TIGR/myocilin protein: Integrity of amino-terminal coiled-coil regions and olfactomedin homology domain is essential for extracellular adhesion and secretion. *Exp. Eye Res. 82*, 1017–1029.

(18) Yam, G. H.-F., Gaplovska-Kysela, K., Zuber, C., and Roth, J. (2007) Sodium 4-phenylbutyrate acts as a chemical chaperone on misfolded myocilin to rescue cells from endoplasmic reticulum stress and apoptosis. *Invest. Ophthalmol. Visual Sci. 48*, 1683–1690.

(19) Jia, L.-Y., Gong, B., Pang, C.-P., Huang, Y., Lam, D. S.-C., Wang, N., and Yam, G. H.-F. (2009) Correction of the disease phenotype of myocilin-causing glaucoma by a natural osmolyte. *Invest. Ophthalmol. Visual Sci. 50*, 3743–3749.

(20) Gobeil, S., Rodrigue, M.-A., Moisan, S., Nguyen, T. D., Polansky, J. R., Morissette, J., and Raymond, V. (2004) Intracellular sequestration of hetero-oligomers formed by wild-type and glaucoma-causing myocilin mutants. *Invest. Ophthalmol. Visual Sci. 45*, 3560–3567.

(21) Powers, E. T., Morimoto, R. I., Dillin, A., Kelly, J. W., and Balch, W. E. (2009) Biological and chemical approaches to diseases of proteostasis deficiency. *Annu. Rev. Biochem. 78*, 959–991.

(22) Kim, B. S., Savinova, O. V., Reedy, M. V., Martin, J., Lun, Y., Gan, L., Smith, R. S., Tomarev, S. I., John, S. W., and Johnson, R. L. (2001) Targeted disruption of the myocilin gene (myoc) suggests that human glaucoma-causing mutations are gain of function. *Mol. Cell. Biol. 21*, 7707–7713.

(23) Lam, D. S., Leung, Y. F., Chua, J. K., Baum, L., Fan, D. S., Choy, K. W., and Pang, C. P. (2000) Truncations in the TIGR gene in individuals with and without primary open-angle glaucoma. *Invest. Ophthalmol. Visual Sci. 41*, 1386–1391.

(24) Resch, Z. T., Hann, C. R., Cook, K. A., and Fautsch, M. P. (2010) Aqueous humor rapidly stimulates myocilin secretion from human trabecular meshwork cells. *Exp. Eye Res. 91*, 901–908.

(25) Mertts, M., Garfield, S., Tanemoto, K., and Tomarev, S. I. (1999) Identification of the region in the N-terminal domain responsible for the cytoplasmic localization of Myoc/Tigr and its association with microtubules. *Lab. Invest. 79*, 1237–1245.

(26) Stamer, W. D., Perkumas, K. M., Hoffman, E. A., Roberts, B. C., Epstein, D. L., and McKay, B. S. (2006) Coiled−coil targeting of myocilin to intracellular membranes. *Exp. Eye Res.83*, 1386–1395.

(27) Hardy, K. M., Hoffman, E. A., Gonzalez, P., McKay, B. S., and Stamer, W. D. (2005) Extracellular trafficking of myocilin in human trabecular meshwork cells. *J. Biol. Chem. 280*, 28917–28926.

(28) Joerger, A. C., and Fersht, A. R. (2008) Structural biology of the tumor suppressor p53. *Annu. Rev. Biochem. 77*, 557–582.

(29) Nordlund, A., and Oliveberg, M. (2008) SOD1-associated ALS: A promising system for elucidating the origin of protein-misfolding disease. *HFSP J. 2*, 354–364.

(30) Liu, M., Hodish, I., Haataja, L., Lara-Lemus, R., Rajpal, G., Wright, J., and Arvan, P. (2010) Proinsulin misfolding and diabetes: Mutant INS gene-induced diabetes of youth. *Trends Endocrinol. Metab. 21*, 652–659.

(31) Grace, M. E., Newman, K. M., Scheinker, V., Berg-Fussman, A., and Grabowski, G. A. (1994) Analysis of human acid β-glucosidase by site-directed mutagenesis and heterologous expression. *J. Biol. Chem. 269*, 2283–2291.

(32) Steet, R. A., Chung, S., Wustman, B., Powe, A., Do, H., and Kornfeld, S. A. (2006) The iminosugar isofagomine increases the activity of N370S mutant acid β-glucosidase in Gaucher fibroblasts by several mechanisms. *Proc. Natl. Acad. Sci. U.S.A. 103*, 13813–13818.

(33) Butters, T. D. (2007) Gaucher disease. *Curr. Opin. Chem. Biol. 11*, 412–418.

(34) Shimizu, S., Lichter, P. R., Johnson, A. T., Zhou, Z., Higashi, M., Gottfredsdottir, M., Othman, M., Moroi, S. E., Rozsa, F. W., Schertzer, R. M., Clarke, M. S., Schwartz, A. L., Downs, C. A., Vollrath, D., and Richards, J. E. (2000) Age-dependent prevalence of mutations at the GLC1A locus in primary open-angle glaucoma. *Am. J. Ophthalmol. 130*, 165–177.

(35) Barnes, M. R. (2010) Genetic variation analysis for biomedical researchers: A primer. *Methods Mol. Biol. 628*, 1–20.

(36) Burns, J. N., Orwig, S. D., Harris, J. L., Watkins, J. D., Vollrath, D., and Lieberman, R. L. (2010) Rescue of glaucoma-causing mutant myocilin thermal stability by chemical chaperones. *ACS Chem. Biol. 5*, 477–487.

(37) Nagy, I., Trexler, M., and Patthy, L. (2003) Expression and characterization of the olfactomedin domain of human myocilin. *Biochem. Biophys. Res. Commun. 302*, 554–561.

(38) Niesen, F. H., Berglund, H., and Vedadi, M. (2007) The use of differential scanning fluorimetry to detect ligand interactions that promote protein stability. *Nat. Protoc. 2*, 2212–2221.

(39) Liu, Y., and Bolen, D. W. (1995) The peptide backbone plays a dominant role in protein stabilization by naturally occurring osmolytes. *Biochemistry 34*, 12884–12891.

(40) Orwig, S. D., and Lieberman, R. L. (2011) Biophysical characterization of the olfactomedin domain of myocilin, an extracellular matrix protein implicated in inherited forms of glaucoma. *PLoS One 6*, e16347.

(41) Alward, W. L., Fingert, J. H., Coote, M. A., Johnson, A. T., Lerner, S. F., Junqua, D., Durcan, F. J., McCartney, P. J., Mackey, D. A., Sheffield, V. C., and Stone, E. M. (1998) Clinical features associated with mutations in the chromosome 1 open-angle glaucoma gene (GLC1A). *N. Engl. J. Med. 338*, 1022–1027.

(42) Adam, M. F., Belmouden, A., Binisti, P., Brezin, A. P., Valtot, F., Bechetoille, A., Dascotte, J. C., Copin, B., Gomez, L., Chaventre, A., Bach, J. F., and Garchon, H. J. (1997) Recurrent mutations in a single exon encoding the evolutionarily conserved olfactomedin-homology domain of TIGR in familial open-angle glaucoma. *Hum. Mol. Genet. 6*, 2091–2097.

(43) Faucher, M., Anctil, J. L., Rodrigue, M. A., Duchesne, A., Bergeron, D., Blondeau, P., Cote, G., Dubois, S., Bergeron, J., Arseneault, R., Morissette, J., and Raymond, V. (2002) Founder TIGR/myocilin mutations for glaucoma in the Quebec population. *Hum. Mol. Genet. 11*, 2077–2090.

(44) Joerger, A. C., and Fersht, A. R. (2007) Structure-function-rescue: The diverse nature of common p53 cancer mutants. *Oncogene 26*, 2226–2242.

(45) Bullock, A., Henckel, J., DeDecker, B., Johnson, C., Nikolova, P., Proctor, M., Lane, D., and Fersht, A. (1997) Thermodynamic stability of wild-type and mutant p53 core domain. *Proc. Natl. Acad. Sci. U.S.A. 94*, 14338–14342.

(46) Bullock, A. N., Henckel, J., and Fersht, A. R. (2000) Quantitative analysis of residual folding and DNA binding in mutant p53 core domain: Definition of mutant states for rescue in cancer therapy. *Oncogene 19*, 1245–1256.

(47) Olivier, M., Langerod, A., Carrieri, P., Bergh, J., Klaar, S., Eyfjord, J., Theillet, C., Rodriguez, C., Lidereau, R., Bieche, I., Varley, J., Bignon, Y., Uhrhammer, N., Winqvist, R., Jukkola-Vuorinen, A., Niederacher, D., Kato, S., Ishioka, C., Hainaut, P., and Borresen-Dale, A. L. (2006) The clinical value of somatic TP53 gene mutations in 1,794 patients with breast cancer. *Clin. Cancer Res. 12*, 1157–1167.

(48) Shaw, B. F., and Valentine, J. S. (2007) How do ALS-associated mutations in superoxide dismutase 1 promote aggregation of the protein? *Trends Biochem Sci. 32*, 78–85.

(49) Seetharaman, S. V., Prudencio, M., Karch, C., Holloway, S. P., Borchelt, D. R., and Hart, P. J. (2009) Immature copper-zinc superoxide dismutase and familial amyotrophic lateral sclerosis. *Exp. Biol. Med. 234*, 1140–1154.

(50) Prudencio, M., Hart, P. J., Borchelt, D. R., and Andersen, P. M. (2009) Variation in aggregation propensities among ALS-associated variants of SOD1: Correlation to human disease. *Hum. Mol. Genet. 18*, 3217–3226.

(51) Bystrom, R., Andersen, P. M., Grobner, G., and Oliveberg, M. (2010) SOD1 mutations targeting surface hydrogen bonds promote amyotrophic lateral sclerosis without reducing apo-state stability. *J. Biol. Chem. 285*, 19544–19552.

(52) Wang, Q., Johnson, J. L., Agar, N. Y., and Agar, J. N. (2008) Protein aggregation and protein instability govern familial amyotrophic lateral sclerosis patient survival. *PLoS Biol. 6*, e170.

(53) Ross, C. A., and Poirier, M. A. (2005) Opinion: What is the role of protein aggregation in neurodegeneration? *Nat Rev. Mol. Cell Biol. 6*, 891–898.

(54) Weiss, M. A. (2009) Proinsulin and the genetics of diabetes mellitus. *J. Biol. Chem. 284*, 19159–19163.

(55) Liu, M., Hua, Q. X., Hu, S. Q., Jia, W., Yang, Y., Saith, S. E., Whittaker, J., Arvan, P., and Weiss, M. A. (2010) Deciphering the hidden informational content of protein sequences: Foldability of proinsulin hinges on a flexible arm that is dispensable in the mature hormone. *J. Biol. Chem. 285*, 30989–31001.

(56) Rozsa, F. W., Shimizu, S., Lichter, P. R., Johnson, A. T., Othman, M. I., Scott, K., Downs, C. A., Nguyen, T. D., Polansky, J., and Richards, J. E. (1998) GLC1A mutations point to regions of potential functional importance on the TIGR/MYOC protein. *Mol. Vision 4*, 20.

(57) Fingert, J. H., Heon, E., Liebmann, J. M., Yamamoto, T., Craig, J. E., Rait, J., Kawase, K., Hoh, S. T., Buys, Y. M., Dickinson, J., Hockey, R. R., Williams-Lyn, D., Trope, G., Kitazawa, Y., Ritch, R., Mackey, D. A., Alward, W. L., Sheffield, V. C., and Stone, E. M. (1999) Analysis of myocilin mutations in 1703 glaucoma patients from five different populations. *Hum. Mol. Genet. 8*, 899–905.

(58) Richards, J. E., Ritch, R., Lichter, P. R., Rozsa, F. W., Stringham, H. M., Caronia, R. M., Johnson, D., Abundo, G. P., Willcockson, J., Downs, C. A., Thompson, D. A., Musarella, M. A., Gupta, N., Othman, M. I., Torrez, D. M., Herman, S. B., Wong, D. J., Higashi, M., and Boehnke, M. (1998) Novel trabecular meshwork inducible glucocorticoid response mutation in an eight-generation juvenile-onset primary open-angle glaucoma pedigree. *Ophthalmology 105*, 1698–1707.

(59) Morissette, J., Clepet, C., Moisan, S., Dubois, S., Winstall, E., Vermeeren, D., Nguyen, T. D., Polansky, J. R., Cote, G., Anctil, J. L., Amyot, M., Plante, M., Falardeau, P., and Raymond, V. (1998) Homozygotes carrying an autosomal dominant TIGR mutation do not manifest glaucoma. *Nat. Genet. 19*, 319–321.

(60) Bruttini, M., Longo, I., Frezzotti, P., Ciappetta, R., Randazzo, A., Orzalesi, N., Fumagalli, E., Caporossi, A., Frezzotti, R., and Renieri, A. (2003) Mutations in the myocilin gene in families with primary open-angle glaucoma and juvenile open-angle glaucoma. *Arch. Ophthalmol. 121*, 1034–1038.

(61) Stone, E. M., Fingert, J. H., Alward, W. L., Nguyen, T. D., Polansky, J. R., Sunden, S. L., Nishimura, D., Clark, A. F., Nystuen, A., Nichols, B. E., Mackey, D. A., Ritch, R., Kalenak, J. W., Craven, E. R., and Sheffield, V. C. (1997) Identification of a gene that causes primary open angle glaucoma. *Science 275*, 668–670.

(62) Vasconcellos, J. P., Melo, M. B., Costa, V. P., Tsukumo, D. M., Basseres, D. S., Bordin, S., Saad, S. T., and Costa, F. F. (2000) Novel mutation in the MYOC gene in primary open glaucoma patients. *J. Med. Genet. 37*, 301–303.

(63) Stoilova, D., Child, A., Brice, G., Desai, T., Barsoum-Homsy, M., Ozdemir, N., Chevrette, L., Adam, M. F., Garchon, H. J., Pitts Crick, R., and Sarfarazi, M. (1998) Novel TIGR/MYOC mutations in families with juvenile onset primary open angle glaucoma. *J. Med. Genet. 35*, 989–992.

(64) Brezin, A. P., Adam, M. F., Belmouden, A., Lureau, M. A., Chaventre, A., Copin, B., Gomez, L., De Dinechin, S. D., Berkani, M., Valtot, F., Rouland, J. F., Dascotte, J. C., Bach, J. F., and Garchon, H. J. (1998) Founder effect in GLC1A-linked familial open-angle glaucoma in Northern France. *Am. J. Med. Genet. 76*, 438–445.

(65) Kanagavalli, J., Pandaranayaka, P. J. E., Krishnadas, S. R., Krishnaswamy, S., and Sundaresan, P. (2007) In vitro and in vivo study on the secretion of the Gly367Arg mutant myocilin protein. *Mol. Vision 13*, 1161–1168.

(66) Hulsman, C. A., De Jong, P. T., Lettink, M., Van Duijn, C. M., Hofman, A., and Bergen, A. A. (2002) Myocilin mutations in a population-based sample of cases with open-angle glaucoma: The Rotterdam study. *Graefe's Arch. Clin. Exp. Ophthalmol. 240*, 468–474.

(67) Mackey, D. A., Healey, D. L., Fingert, J. H., Coote, M. A., Wong, T. L., Wilkinson, C. H., McCartney, P. J., Rait, J. L., de Graaf, A. P., Stone, E. M., and Craig, J. E. (2003) Glaucoma phenotype in pedigrees with the myocilin Thr377Met mutation. *Arch. Ophthalmol. 121*, 1172–1180.

(68) Alward, W. L., Kwon, Y. H., Khanna, C. L., Johnson, A. T., Hayreh, S. S., Zimmerman, M. B., Narkiewicz, J., Andorf, J. L., Moore, P. A., Fingert, J. H., Sheffield, V. C., and Stone, E. M. (2002) Variations in the myocilin gene in patients with open-angle glaucoma. *Arch. Ophthalmol. 120*, 1189–1197.

(69) Melki, R., Belmouden, A., Brezin, A., and Garchon, H. J. (2003) Myocilin analysis by DHPLC in French POAG patients: Increased prevalence of Q368X mutation. *Hum. Mutat. 22*, 179.

(70) Pei, J., Kim, B. H., Tang, M., and Grishin, N. V. (2007) PROMALS web server for accurate multiple protein sequence alignments. *Nucleic Acids Res. 35*, W649–W652.